

## Effect of mechanical milling on the corrosion behavior of Al–Zn/Al<sub>2</sub>O<sub>3</sub> composite in NaCl solution

T. G. Durai · Karabi Das · Siddhartha Das

Received: 13 October 2006 / Accepted: 26 March 2007 / Published online: 9 June 2007  
© Springer Science+Business Media, LLC 2007

**Abstract** Ceramic particle reinforced aluminum metal matrix composites (MMCs) have resulted in potential use in aerospace and automobile industries. The composites have been processed by mechanical milling followed by traditional powder metallurgy route. The Al crystallite size is reduced to 27 nm after 60 h of milling. Results of the corrosion tests, evaluated using the potentiodynamic method in the NaCl solution, indicate that corrosion of the investigated composite materials depends on the weight fraction of the reinforcing particles. It has been found out, based on the determined anode polarization curves, that the investigated materials are susceptible to pitting corrosion. Moreover, experimental results suggest that the milled composite material Al–Zn/Al<sub>2</sub>O<sub>3p</sub> has higher corrosion resistance in the selected environment compared to unmilled composite Al–Zn/Al<sub>2</sub>O<sub>3p</sub>. Polarization curves show that the milling procedure improves the composite corrosion resistance in passive conditions. This is illustrated by the corrosion potential, which becomes nobler with milling.

### Introduction

Aluminum metal matrix composites are attractive for many applications in chemical, automobile and aerospace industries because of their high strength-to-weight ratio, high thermal conductivities, and good resistance to degradation in some corrosive environments. Many high-

performances, particle-dispersed aluminum alloys have been developed with significantly improved mechanical properties, leading to extended applications [1]. Nanocrystalline materials may be produced in a number of ways, e.g., gas condensation, spray conversion, ball milling and electrochemical deposition. Mechanical milling (MM) is a high-energy ball milling technique, which has been established as a prominent route for the synthesis of a variety of advanced materials including nanocrystalline materials.

The potential use of nanocrystalline materials in structural application due to the hardening of polycrystalline material through the refinement of their grain size has led to the development of various deformation techniques for the fabrication of nanocomposites [2, 3]. Mechanical milling has proved to be an ideal method for the preparation of particle reinforced MMCs. It has been recognized that mechanical milling can be used to induce Chemical (displacement) reactions at much lower temperature than normally required. This allows for the in situ formation of different hardening phases during milling or subsequent thermal processing of the milled powders [4].

These materials are expected to exhibit good corrosion resistance in the aggressive environment. Therefore, determination of the corrosion resistance of composite materials with aluminum matrix reinforced with ceramic additives is quite important [5]. Aluminum and its alloys generally have good corrosion resistance under atmospheric conditions. Thin and strongly adhering aluminum oxide layer, developed spontaneously, provides a protection and slows down the electrochemical corrosion process. However, the investigations of the composite materials having the aluminum matrix reinforced with Al<sub>2</sub>O<sub>3</sub> have suggested the possibility of occurrence of the selective corrosion at the interface between the ceramic and the matrix phases [6]. It has been reported that the Al<sub>2</sub>O<sub>3</sub>

T. G. Durai · K. Das (✉) · S. Das  
Department of Metallurgical and Materials Engineering, Indian  
Institute of Technology, Kharagpur 721302, India  
e-mail: karabi@metal.iitkgp.ernet.in

ceramic particles cause the decrease in the corrosion resistance of the investigated material [5].

In the current work alumina reinforcements have been produced by the mechano chemical reaction between Al and ZnO. Initial milling of the mixed powders produces a homogeneous mixture of the powders. Ball milling has resulted in the refinement of the grains resulting in nano-sized powders. XRD analyses of the milled samples have been carried out to determine the phase transformation taking place during milling. Corrosion behaviors of the samples have been evaluated.

## Experimental procedure

### Processing of MMCs

The materials used in this study are aluminum powders (Loba Chemie, 99.7% purity, <20 $\mu$ m size) and ZnO powders (Loba Chemie, 99.5% purity, <10  $\mu$ m size). Powder mixtures (Al–10wt%ZnO and Al–20wt%ZnO) have been subjected to a high-energy ball milling using a Fritsch Pulverisette-5 mill with tungsten balls and vials. Tungsten carbide balls with a diameter of 10 mm have been used to mill the powder using a ball to powder weight ratio of 10:1 up to 60 h. Milling has been carried out at 300 rpm using toluene medium in order to avoid oxidation or sticking of powder on the walls of the vial. Samples have been taken out from the vial from time to time during milling. Mechanically milled samples have been characterized by Phillips X-pert system diffractometer with a Co K $\alpha$  radiation. The crystallite size and lattice strain in the powder particles can be determined using the x-ray peak broadening techniques. X-ray peak broadening is due to (a) instrumental effects, (b) small particle size, and/or (c) lattice strain in the material. Using the Scherrer formula one determines the crystallite size. The powders have been cold pressed under 650 MPa to form green compacts with a diameter of 10 mm followed by heating to a particular temperature to initiate the reaction. The pellets have been sintered at 610  $^{\circ}$ C for 3 h under flowing argon.

### Electrochemical corrosion tests

The potentiodynamic polarization studies have been configured in a cell using three-electrode assembly with a saturated calomel reference electrode, a platinum counter electrode and the composite material as the working electrode. The inspected surfaces of the specimens have been cleaned with acetone immediately before the examinations. The electrolyte solution contains 3.5% (by weight) NaCl in distilled water. This solution has a measured pH of  $\sim$ 6. The surface area of the examined specimens is about 0.81 cm $^2$ .

The tests have been carried out at room temperature. Before the potentiodynamic tests the samples have been allowed to stabilize at their corrosion potential for at least 300 s. The measurements are made at a scan rate of 1 mV/s using AUTOLAB 30 PG Stat (Netherlands). The results reported in this paper are an average of at least three corrosion tests. Surface morphology of the corroded samples has been studied using scanning electron microscope (Joel JSM 5800 analyzer).

## Results and discussion

### XRD analysis

The XRD patterns of the Al–ZnO powder mixtures, milled for different times, are presented in Fig. 1. It can be seen that the intensities of the Al and ZnO peaks decrease with increasing milling time. The XRD patterns of some milled samples consist of the diffraction lines of alumina, which

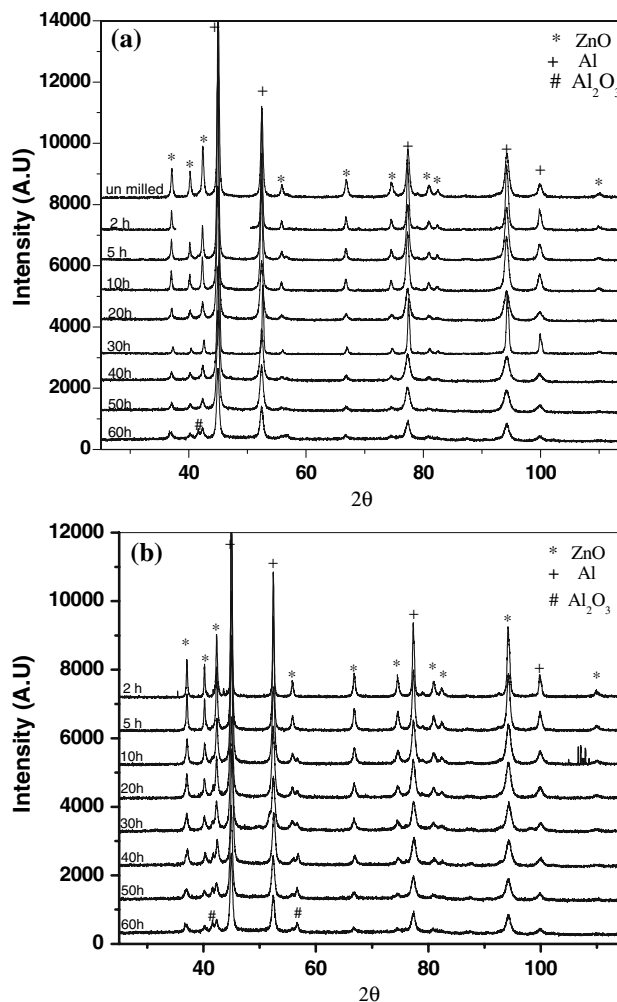


**Fig. 1** XRD patterns (a) Al–10ZnO and (b) Al–20ZnO mixture as a function of milling time

formed “*in situ*” directly during the milling process. It is worthwhile to notice that this phase transformation has been accompanied by an increase in the temperature of the vial, i.e., a combustion-type reaction has taken place. The Al<sub>2</sub>O<sub>3</sub> peak with a high intensity evolves as a shoulder of ZnO peak near 42.30°.

Nanocrystalline powders are obtained as a result of continuous fracture process during milling. The approximate size of the nanocrystalline powders has been calculated using the full width half maximum of the Al peaks and Scherrer formula. With an increase in milling time the broadening of the peak is observed indicating a refinement of the crystallite size. It has been shown in Fig. 2 that the crystallite size decreases continuously with an increase in milling time. Nanocrystalline powders of approximately 27 nm size are obtained after 60 h of milling. It can be seen that with an increase in milling time lattice strain increases. Increase in lattice strain is commonly attributed to plastic deformation [7].

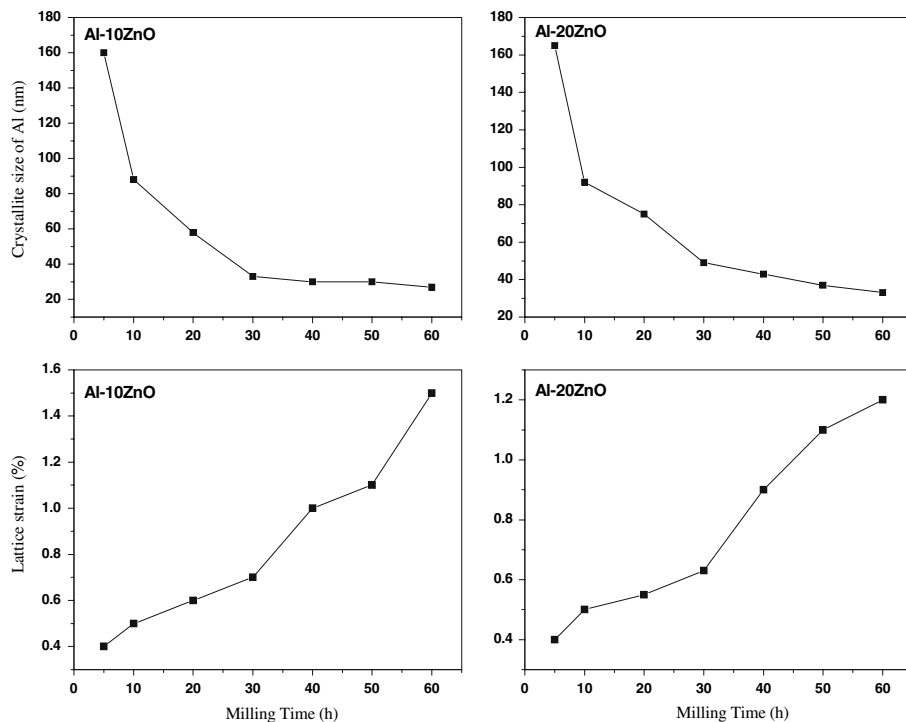
The Fig. 3 shows the XRD pattern of Al–10ZnO powder milled for 60 h and then sintered at 610 °C for 3 h. It can be seen that after sintering none of the ZnO peaks are present. It can be inferred that ZnO has been reduced during sintering and the reduced Zn has goes to solid solution of Al (Zn).

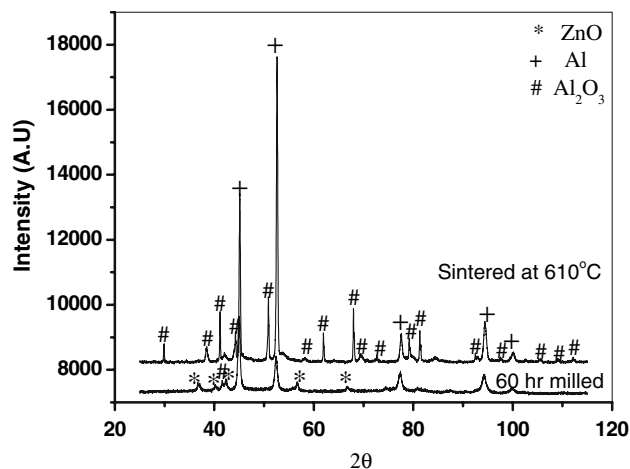
Electrochemical behavior

Al–10ZnO milled material exhibits the lowest corrosion current of 0.0042 mA/cm<sup>2</sup> in the passive range and the

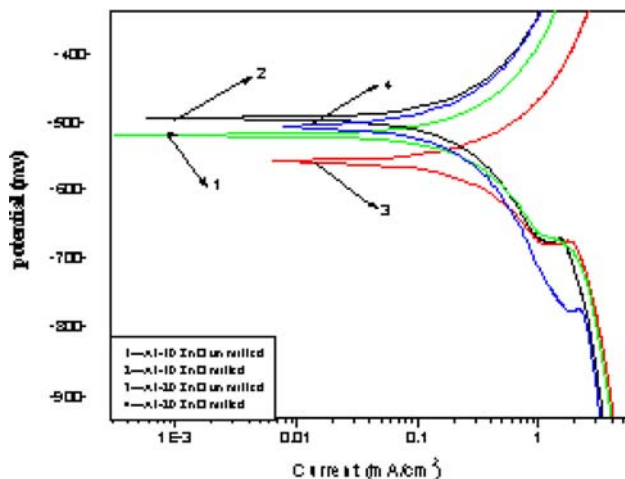
highest value of polarization resistance of 934 Ω/cm<sup>2</sup>, suggesting attractive corrosion resistance in the 3.5 wt% NaCl solution compared to other materials. The variation of the open circuit potential (OCP) with the immersion time in 3.5 wt% NaCl solution for unmilled and 60 h milled working electrodes is presented in Fig. 4. The change in OCP is assumed to be related to the growth of the passive layer on the sample. For unmilled sample, OCP value is comparatively in more active side. For milled sample, the open circuit potential starts at a more positive value and increases more drastically during the 300 s. The larger OCP variation for milled sample may indicate a greater reactivity with the electrolyte to form the passive layer. The significantly nobler OCP value for milled sample in the initial state as well as in the near steady state illustrates the positive effect of the ball milling process on the corrosion resistance of samples. Figure 4 shows typical polarization curves of unmilled and 60 h milled samples in 3.5 wt% NaCl solution. The curves have a similar shape and no active–passive transition is observed on the anodic part of the polarization curves, confirming the passive behavior of Al independent of its microstructures in 3.5 wt% NaCl solution. However, a significant shift in the positive direction of the corrosion potential is observed with the milled samples. The corrosion parameters deduced from polarization measurements in 3.5wt%NaCl solution are summarized as a function of the milling time in Table 1. It shows that the corrosion potential ( $E_{corr}$ ) becomes more positive with milling. The corrosive behavior of nanostructured materials has received only

Fig. 2 Crystallite size and Lattice Strain of Al as a function of milling time





**Fig. 3** XRD patterns of Al–10ZnO



**Fig. 4** Polarization plots for (unmilled and 60 h milled) sintered samples

limited attention. Thus, it becomes difficult to predict the electrochemical behavior of these materials from the properties of their coarse-grained. It has been reported that the linear sweep voltammograms of pure nanocrystalline palladium obtained by a sputtering process presented a

current density higher than that of a pure microcrystalline one [8]. This performance is owing to a poor consolidation of mechanically milled powders and the existence of a high stored energy originated by the nanocrystalline grain size and the accumulation of the other crystal defects formed during the ball milling of the powders [9]. In the present case, the materials have been sintered at low temperatures to release the stored energy and improve the corrosion resistance of the materials.

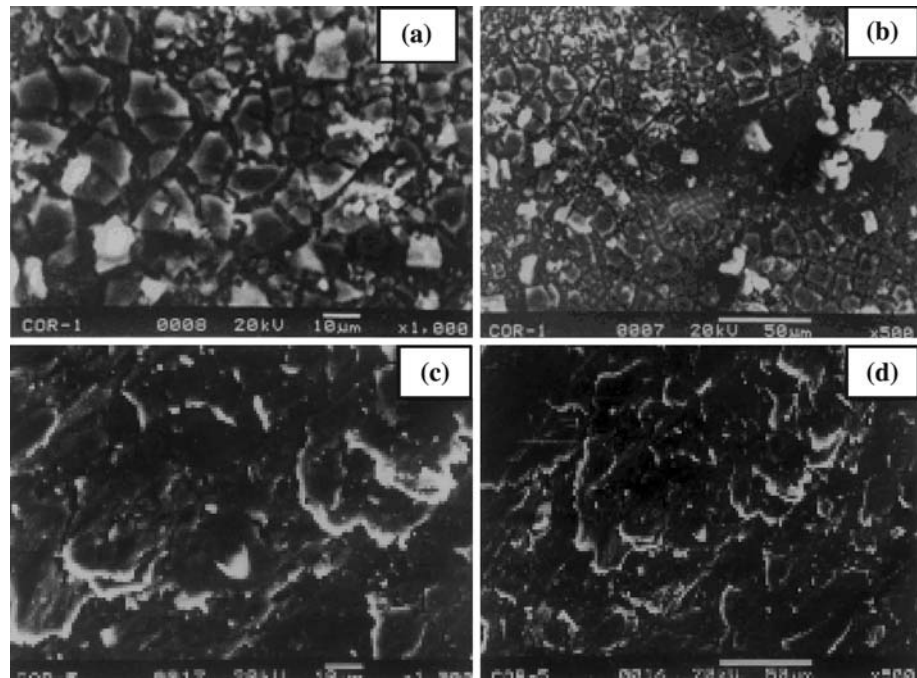
From the scanning electron micrographs of Fig. 5, it appears that the corroded polycrystalline samples display a few large, deep pits, while the corroded nanocrystalline samples show a multitude of smaller pits. This result agrees with the contention that corrosion is concentrated at triple junctions and grain boundaries. The polycrystalline sample, having very large grains, has proportionally very few atoms located in triple junctions or grain boundaries. Corrosion, when localized at these sparse locations, tends to result in large, deep pits. As the grain size decreases, the number of triple junctions and grain boundaries increases. Hence, the number of pits increases while their size tends to decrease. Both samples exhibit extensive corrosion, but the nanocrystalline samples are more uniformly corroded while the specimen with larger grain size shows extensive localized attack along the grain boundaries and triple junctions. Pitting is more prominent in Al–20ZnO than in Al–10ZnO in the 3.5 wt%NaCl solution. However, the highest corrosion current value of 0.0063 mA/cm<sup>2</sup> is observed for the composite material Al–20ZnO, which attests to its low corrosion resistance. Also polarization resistance for this composite is the lowest (875 Ω/cm<sup>2</sup>) testifying its less corrosion resistance compared to other investigated here. The micrographs of the specimens after the corrosion tests confirm the influence of volume fraction of ceramics particles on corrosion resistance.

It is known that metal matrix composites can provide significantly improved structural and mechanical properties compared to metals and alloys. There are reports that some Al based MMCs are inferior to the corresponding matrix alloys due to precipitates and matrix-reinforcement interfaces in the composites [10]. Most of the studies indicate

**Table 1** Results of electrochemical corrosion investigation

Material	Milling Time (h)	Sintering Temp (°C)	Corrosion potential, $E_{cor}$ (mV)	Corrosion current, $i_{cor}$ (mA/cm <sup>2</sup> )	Polarization resistance, $R_p$ (Ω/cm <sup>2</sup> )	Corrosion rate, $v_{cor}$ (mm/y)
Al	Unmilled	600	–653	0.0163	744	0.209
Al–10ZnO	Unmilled	950	–517	0.0101	802	0.165
Al–10ZnO	60 hr	610	–480	0.0042	934	0.095
Al–20ZnO	Unmilled	950	–572	0.0156	780	0.180
Al–20ZnO	60 hr	610	–500	0.0063	875	0.112

**Fig. 5** Microstructure of the sintered samples after corrosion test: (a) unmilled Al–10ZnO, (b) unmilled Al–20ZnO, (c) 60 h-milled Al–10ZnO and (d) 60 h-milled Al–20ZnO



that Al MMCs reinforced with ceramic phases in the form of particles, whiskers, or fibers exhibit high resistance to corrosion [11]. Nanocrystalline materials provide a better localized corrosion resistance resulted owing to evenly distributed corrosion current. It has been found that nanocrystalline metals have corroded more generally on all exposed surfaces, while polycrystalline metals with grain size in the micro meter range have suffered severe localized corrosion.

In this study it has been found that the aluminum matrix composites with nano-size reinforcement offer better corrosion resistance than the matrix material. The matrix grain size is in the micrometer range. Following discussion is necessary to understand this observation. The corrosion behavior of MMCs depends on various factors like compositions of the alloy used and the reinforcing particles, their size and distribution in the matrix, and the nature of the interface between the matrix and the reinforcement [12]. After the corrosion test, each sample was cleaned thoroughly and weighed, and their weight loss is reported in Table 2. In the present case the weight loss is encountered in the composites as well as in the base metal, and

this is predominately due to the formation of corrosion pits on the surface. In the case of the base metal, the strength of the acid used causes the crack formation on the surface, which eventually leads to the formation of more severe pits, thereby causing the loss of the material. Since, there is no reinforcement provided in the base metal, it fails to provide resistance to the acidic medium regarding crack formation. Hence, the weight loss in the unreinforced metal is higher than that in the composites.

Alumina being ceramic remains inert in the acid and it is hardly affected by the acidic medium. Though the weight loss is lesser than that of the base metal, the composites also show the formation of pits on the surface. The number of pits gets decreased with the addition of nanocrystalline alumina compared to that in the base metal. There is the evidence for the presence of only pits, but not the cracks in the composites. This supports the effects of reinforcing nano-size alumina particles in improving the corrosion resistance of the composites. The alumina particles resist the severity of the acid attack to a certain extent and hence the formation of the cracks. There is hardly any information available in the literature. Experiments were repeated four times for each sample and the same trend was observed every time. This appears to be the most logical explanation available at this time to explain our observation.

**Table 2** The weight loss owing to the electrochemical corrosion

Material	Milling Time (h)	Weight Loss (mg)
Pure aluminum	Unmilled	5.2
Al–10ZnO	Unmilled	3.5
Al–10ZnO	60 h	2.7
Al–20ZnO	Unmilled	4.3
Al–20ZnO	60 h	3.0

## Conclusions

1. Mechanical milling improves the distribution of alumina particles throughout the matrix and decreases the

reinforcement particle size. The average crystallite size obtained in this study is approximately 27 nm.

2. Heavy deformation of Al particles during milling increases the internal energy, which acts as a driving force during sintering and enhances the formation of Al<sub>2</sub>O<sub>3</sub> particles.
3. The corrosion current of nanocrystalline composite is found to decrease with an increase in milling time. This maybe attributed to the high degree of surface defects resulting from the high surface fractions of grain boundaries and triple junctions. This leads to the rapid formation of a stable and uniform passive film, responsible for the high corrosion resistance. Whereas conventional polycrystalline composites are more susceptible to localized corrosion.
4. This study reveals that ball milling may induce improved corrosion resistance in some materials.

**Acknowledgement** The financial support received from the Department of Science and Technology, Government of India, is gratefully acknowledged.

## References

1. Datta J, Datta S, Banerjee MK, Bandyopadhyay S (2004) Composites: Part A 35:1003
2. Aikin RM Jr (1997) J Organomet 49:35
3. Koczak MJ, Premkumar MK (1993) J Min Met Mater Soc 45(1):44
4. Ying DY, Zhang DL (2000) Mater Sci Eng A 286:152
5. Dobrzański LA, Włodarczyk A, Adamiak M (2005) J Mater Process Technol 162:27
6. Kiourtsidis GE, Skolianos SM, Pavlidou EG (1999) Corros Sci 41:1185
7. Grosjean M-H, Zidoune M, Roue L, Huot J, Schulz R (2004) Electrochimica Acta 49:2461
8. Kirchheim R, Huang XY, Cui P, Birringer R, Gleiter H (1992) Nanostruct Mater 1:167
9. Elkedim O, Cao HS, Guay D (2002) J Mater Process Technol 121:383
10. Ashassi-Sorkabi H, Ghasemi Z, Seifzadeh D (2005) Appl Surf Sci 249:408
11. Badawy WA, Al-Kharafi L FM (1997) Corr Sci 39(4):681
12. Sharma SC, Somashekar DR, Satish BM (2001) J Mater Process Technol 118:62